Journal of Biomolecular NMR, **23:** 227–238, 2002.
KLUWER/ESCOM

REDOR: An assessment of the efficacy of dipolar recoupling with adiabatic inversion pulses

Jörg Leppert, Bert Heise, Matthias Görlach & Ramadurai Ramachandran*
Abteilung Molekulare Biophysik/NMR-Spektroskopie, Institut für Molekulare Biotechnologie, 07745 Jena, Germany

Received 14 June 2002; Accepted 20 June 2002

Abstract

A numerical assessment of the efficacy of REDOR recoupling of heteronuclear dipolar interactions employing adiabatic dephasing pulses has been carried out by considering an isolated dipolar coupled spin 1/2 I-S system. At moderate magic angle spinning frequencies in the range of 3–6 kHz and when the CSA of the dephased spins is large, it is shown that efficient broadband heteronuclear dipolar recoupling and reliable distance estimates can be achieved even under conditions where a significant fraction of the rotor period is occupied by the adiabatic pulse. The efficacy of REDOR with adiabatic inversion pulses has been demonstrated experimentally in two model ^{15}N-^{13}C spin systems, (^{13}C′,^{15}N) Aib-(^{15}N) Aib-NH_2 (Aib = α-aminoisobutyric acid) and (1-^{13}C,^{15}N) glycine.

Introduction

The advent of hetero- and homonuclear dipolar recoupling techniques (Bennett et al., 1994; Griffin, 1998; Dusold and Sebald, 2000) has opened up the possibilities for the convenient measurement of distance and orientational parameters in biomolecular systems under magic-angle spinning conditions. Heteronuclear dipolar recoupling techniques such as REDOR (Gullion and Schaefer, 1989a, b) and TEDOR (Hing et al., 1992, 1993, Fujiwara et al., 1995) and homonuclear dipolar recoupling sequences such as RFDR (Bennett et al., 1992, 1998; McDermott et al., 2000; Pauli et al., 2000) employ 180° inversion pulses to achieve dipolar recoupling. TEDOR and RFDR also provide an approach for achieving hetero- and homonuclear 2D chemical shift correlation of dipolar coupled spins. Typically, dipolar recoupling experiments are carried out using conventional rectangular 180° pulses and the recoupling 180° pulses are applied with suitable x- and y-phase alternation (Gullion et al., 1990) to compensate for H_1 inhomogeneity and resonance offset effects (Gullion and Schaefer, 1991; Naito et al., 1996; Chan et al., 2000; Nishimura et al., 2001; Jaroniec et al. 2001). In dipolar recoupling experiments, e.g., REDOR, application of adiabatic inversion pulses (Baum et al., 1985; Kupce and Freeman, 1995, 1996; Tannus and Garwood, 1996; Hwang et al., 1998), instead of the conventional rectangular 180° pulses, provides an alternative approach for the elimination of the deleterious effects of H_1 inhomogeneity and resonance offset. This is seen from our recent REDOR studies with adiabatic inversion pulses which dealt with the extraction of ^{15}N and ^{13}C chemical shift tensor orientations from spinning sideband intensities (Heise et al., 2000; J. Leppert et al., unpublished). The accurate extraction of orientational data requires the analysis of the intensities of a sufficient number of spinning sidebands (Goetz et al., 1997; Leppert et al., 2000a, b, 2001; Heise, 2001; J. Leppert, 2001; Heise et al., 2001; O'Connor et al., 2002). Consequently, these REDOR experiments were typically carried out at low spinning speeds of 1–2 kHz. It was seen experimentally that the results obtained employing adiabatic pulses were in agreement with those expected from ideal 180° pulses (Heise et al., 2000; J. Leppert et al., unpublished). This is not surprising as at low spinning speeds the adiabatic pulses employed were occupying only a small fraction (∼ 10%) of the rotor period, although they were of much larger duration compared to

*To whom correspondence should be addressed. E-mail: raman@imb-jena.de

typical rectangular 180° pulses. Additionally, only a small number of rotor periods of dipolar recoupling is typically used for the measurement of chemical shift tensor orientations. However, most of the REDOR distance measurements reported in the literature have been carried out with several rotor periods of dipolar recoupling and in the spinning range of 3–6 kHz. For REDOR distance measurements, no assessment of the efficacy of dipolar recoupling with adiabatic inversion pulses has been carried out till date.

An adiabatic pulse is defined by the form of the amplitude modulation and frequency sweep profile. Many different modulation functions have been proposed (Baum et al., 1985; Kupce and Freeman, 1995, 1996; Tannus and Garwood, 1996; Hwang et al., 1998). Adiabatic inversion pulses with long duration typically require less RF power to satisfy the adiabatic sweep requirements. Pulses with long duration will be required in order to minimise the average power dissipated in the probe in experiments with long dipolar mixing times or in cases where RF transmitter power is limited. Even at moderate spinning speeds of 3–6 kHz, adiabatic pulses may occupy a significant fraction of the rotor period. In the context of rectangular 180° pulses, Jaroniec et al. (2000) have analysed the REDOR recoupling of heteronuclear dipolar interactions at high magic-angle spinning frequencies and as a function of the ratio of the rectangular 180° pulse width, τ_p to the rotor period,τ_r, $\chi = (2\tau_p/\tau_r)$. Employing the xy-4 phasing scheme (Gullion et al., 1990; Gullion and Schaefer, 1991) and neglecting resonance offsets, CSAs and H_1 inhomogeneity it was found that the dipolar recoupling behaviour with rectangular pulses deteriorates only marginally for values of χ less than 0.6. It is worth mentioning that the resonance offset effects arising from large CSAs do not get eliminated in the spinning regime of 3–6 kHz typically employed in REDOR studies. It has been reported recently (Jaroniec et al., 2001) that with increasing CSA of the dephased spins, the REDOR dephasing curves for all phasing schemes deviate from ideal behaviour and the response obtained with the xy-4 phasing scheme approaches most closely the ideal curve. In view of the potential utility of adiabatic inversion pulses for eliminating H_1 inhomogeneity and resonance offset effects in REDOR distance measurements, we have carried out, without neglecting resonance offsets, CSAs and H_1 inhomogeneity, a numerical assessment of the efficacy of REDOR recoupling of dipolar interactions with adiabatic pulses. Our studies indicate that, in the presence of a large CSA of the dephased spins, efficient broadband heteronuclear dipolar recoupling and reliable distance estimates can be obtained with adiabatic inversion pulses. Experimental ^{15}N-^{13}C REDOR measurements with adiabatic inversion pulses have also been carried out on model systems.

Numerical simulations

To analyse the effect of the adiabatic pulse width on the efficacy of REDOR recoupling, we have used the pulse sequence given in Figure 1. The adiabatic 180° pulses are applied in the dephasing channel with only one rectangular 180° pulse (assumed to be ideal here) applied on the observe channel to refocus chemical shift evolution. With the sequence given in Figure 1, one has effectively two adiabatic pulses per rotor period. In this study we have mainly employed the tanh/tan adiabatic inversion pulse (Hwang et al., 1998) constructed from the following adiabatic half passage and its time reversed half passage:

$$\omega_1(t) = \omega_1(\max)\tanh\left[\xi 2t/T_p\right],$$

$$\Delta\omega(t) = \Delta\omega_{max}\left[\tan(\kappa(1-2t/T_p))\right]/\tan(\kappa),$$

where $\xi = 10$, $\tan(\kappa) = 20$ and $0 \le t \le T_p/2$. Additionally, to assess the dependence of the dipolar recoupling efficiency on the nature of the adiabatic pulse profile, we have also employed the constant adiabaticity inversion pulse 'cagauss' defined by the modulation profiles:

$$\omega_1(t) = \omega_1(\max)\exp(-\beta t^2),$$

$$\Delta\omega(t) = \lambda\,\mathrm{erf}(\beta t),$$

where λ and β are defined as

$$\lambda = [\omega_1(\max)]^2/\beta Q$$

and

$$\beta = (1/\tau)\sqrt{-\ln(a_{tr})},$$

where Q is the adiabaticity parameter (Kupce and Freeman, 1996) and a_{tr} is the truncation parameter ($0 < a_{tr} < 1.0$). A Q value of 4 and $a_{tr} = 0.01$ were employed in this work. The frequency sweep is implemented in the spectrometer hardware as a phase modulation, $\phi(t) = \int \Delta\omega(t)\,dt$. Unlike the cagauss inversion pulse, the tanh/tan pulse does not have a constant Q value within the effective sweep bandwidth and far from resonance, the tanh/tan pulse

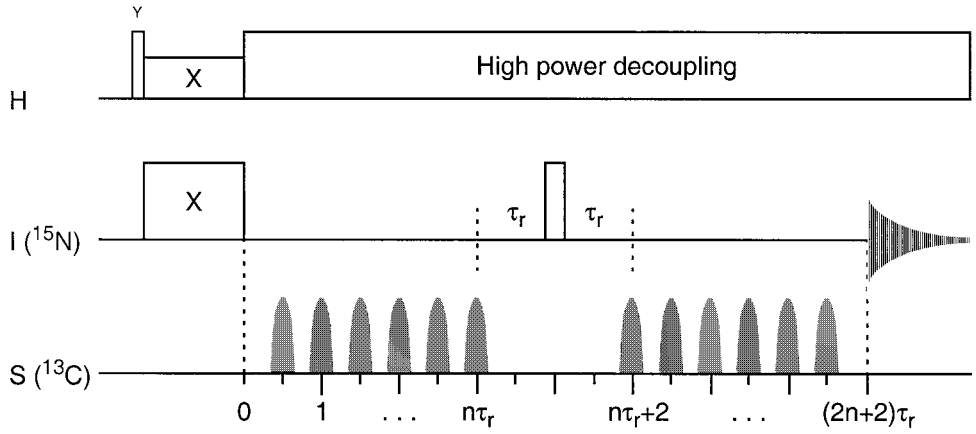

Figure 1. REDOR pulse sequence employed in this work. The ^{15}N-^{13}C dipolar interaction is recouped by applying rotor synchronised adiabatic inversion pulses in the dephasing channel.

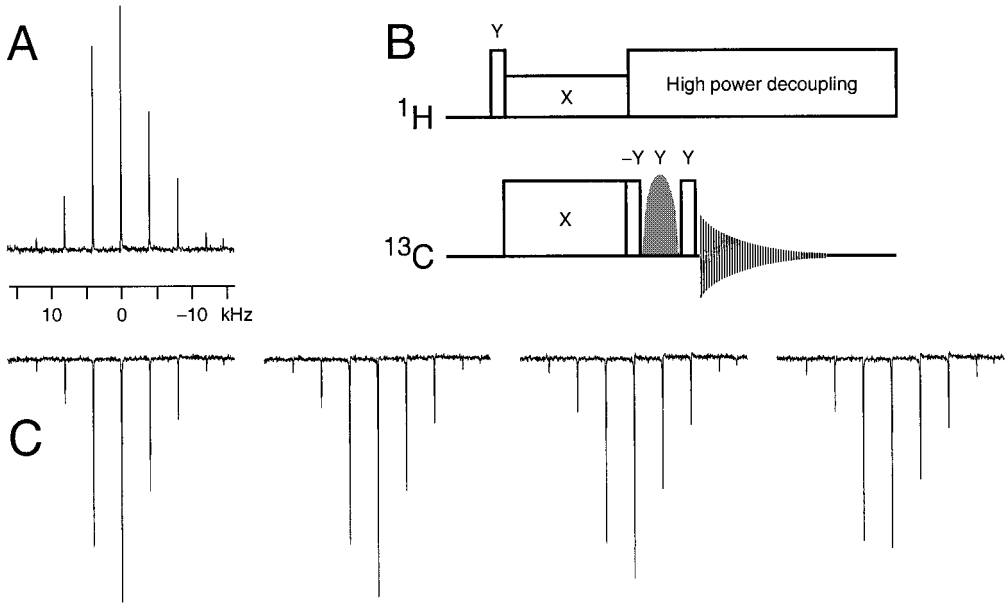

Figure 2. (A) ^{13}C CPMAS spectrum, at a spinning speed of 4000 Hz, of the AibAib dipeptide sample. (B) pulse sequence employed for assessing the inversion characteristics of the adiabatic pulses. (C) ^{13}C spectra of the dipeptide obtained employing this sequence. 40 μs tanh/tan adiabatic pulses were employed with RF field strengths of 50, 44.5, 39.7 and 35.4 kHz (left to right). All tanh/tan adiabatic pulses employed in this work had an *R* value, representing the product of the pulse bandwidth and the pulse length (Hwang et al., 1998), of 60.

employs very fast frequency sweeps. With the typical transmitter power available, it is possible to generate tanh/tan inversion pulses of short duration and with good broadband inversion characteristics as shown in Figure 2. We have employed tanh/tan pulses with a duration in the range of 40–70 μs. The cagauss pulses uniformly had a duration of 80 μs and an RF field strength of ∼50 kHz. Figure 3 shows contour plots of the observed I_z magnetisation, as a function of RF field strength and resonance offset, after the application of the inversion pulses employed. These plots were generated considering a single spin 1/2 system and neglecting CSA. Over the ^{13}C spectral range to be excited by the adiabatic inversion pulse (approximately ±12 kHz), it is seen from Figure 3 that the minimum RF power required to achieve satisfactory nuclear spin inversion gets reduced with tanh/tan pulses of longer duration. Figure 3 also shows the inversion profiles of the cagauss and a 9 μs rectangu-

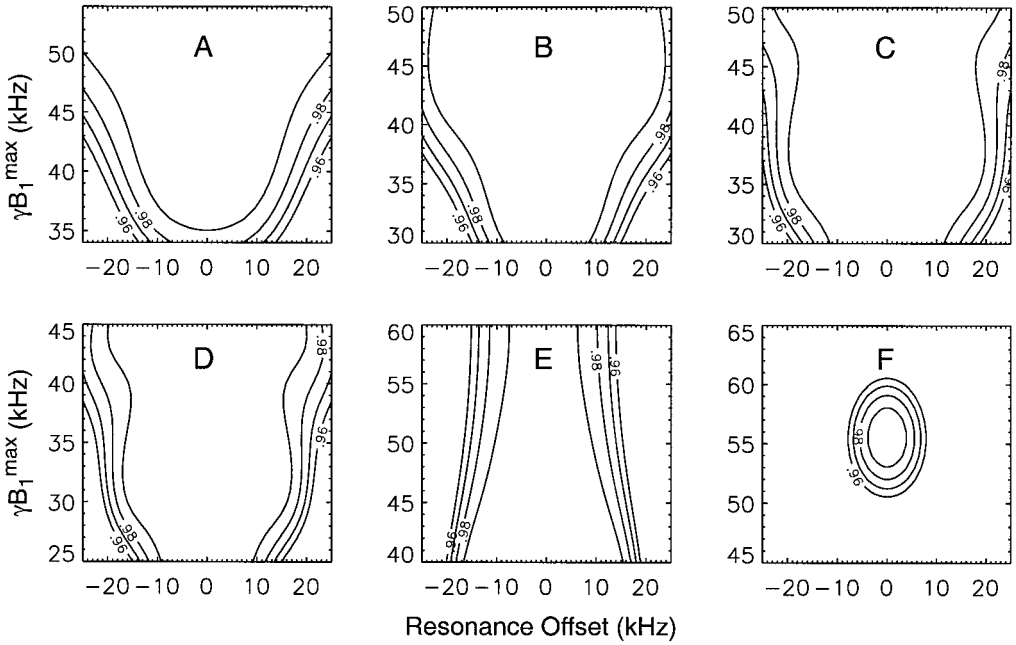

Figure 3. Contour plots of $\langle -I_z \rangle$ (expressed as a fraction of the initial magnetisation) after the inversion pulse. The plots A, B, C and D were generated for a tanh/tan pulse of 40, 50, 60 and 70 μs duration, respectively. The plots given in E and F were generated for the cagauss adiabatic pulse of 80 μs and for a rectangular 180° pulse of 9 μs duration, respectively.

lar 180° pulse. The superior inversion profiles of the adiabatic pulses are clearly apparent.

For simulating the REDOR response with adiabatic pulses, we have considered an isolated, dipolar coupled I-S heteronuclear spin 1/2 pair. The total Hamiltonian in the rotating frame is defined as

$$\mathcal{H}(t) = \mathcal{H}_A + \mathcal{H}_B(t) + \mathcal{H}_C(t), \qquad (1)$$

where

$$\mathcal{H}_A = \omega_I^{iso} I_z + \omega_S^{iso} S_z,$$

$$\mathcal{H}_B(t) = \omega_I^{aniso}(t) I_z + \omega_S^{aniso}(t) S_z + \omega_d(t) I_z S_z$$

and

$$\begin{aligned} \mathcal{H}_C(t) &= \omega_{1I}[I_x \cos\phi + I_y \sin\phi] \\ &\quad + \omega_{1S}(t)[S_x \cos\Phi(t) + S_y \sin\Phi(t)] \end{aligned}$$

represent the contribution to the Hamiltonian from the isotropic chemical shift, anisotropic chemical shift and dipolar interactions and the RF irradiation. With the total spin Hamiltonian given by Equation 1, the evolution operator of the spin system is given by

$$U(t) = T \exp\left[-i \int_0^t \mathcal{H}(t')\, dt'\right],$$

where T is the Dyson time-ordering operator. For the calculation of the propagator during the application of an adiabatic pulse, the RF pulse is divided into a finite number of time slices of equal duration (200 in our case), with each slice characterised by a proper amplitude and phase so as to mimic the required amplitude and frequency modulation. All anisotropic interaction Hamiltonians are assumed to vary only from one time slice to another. The time dependence of the anisotropic Hamiltonians during the individual time slices is neglected. The propagators corresponding to the individual time slices are calculated via numerical diagonalisation of the Hamiltonian matrix. The total evolution operator for the entire adiabatic pulse is then calculated by a time-ordered product of the evolution operators corresponding to the individual time slices. For each crystallite orientation, the propagators for the adiabatic pulses applied at the middle and end of the rotor period are calculated separately and used for the REDOR response calculation. The observed REDOR signal is finally calculated via

$$\begin{aligned} \langle I^+ \rangle &= \mathrm{Tr}[I^+ \sigma(t_i)] \\ &= \mathrm{Tr}[I^+ U(t_i)\, \sigma(0) U^{-1}(t_i)], \end{aligned}$$

where $\sigma(t_i)$ is the density matrix at time t_i during data acquisition. All simulations were carried out with

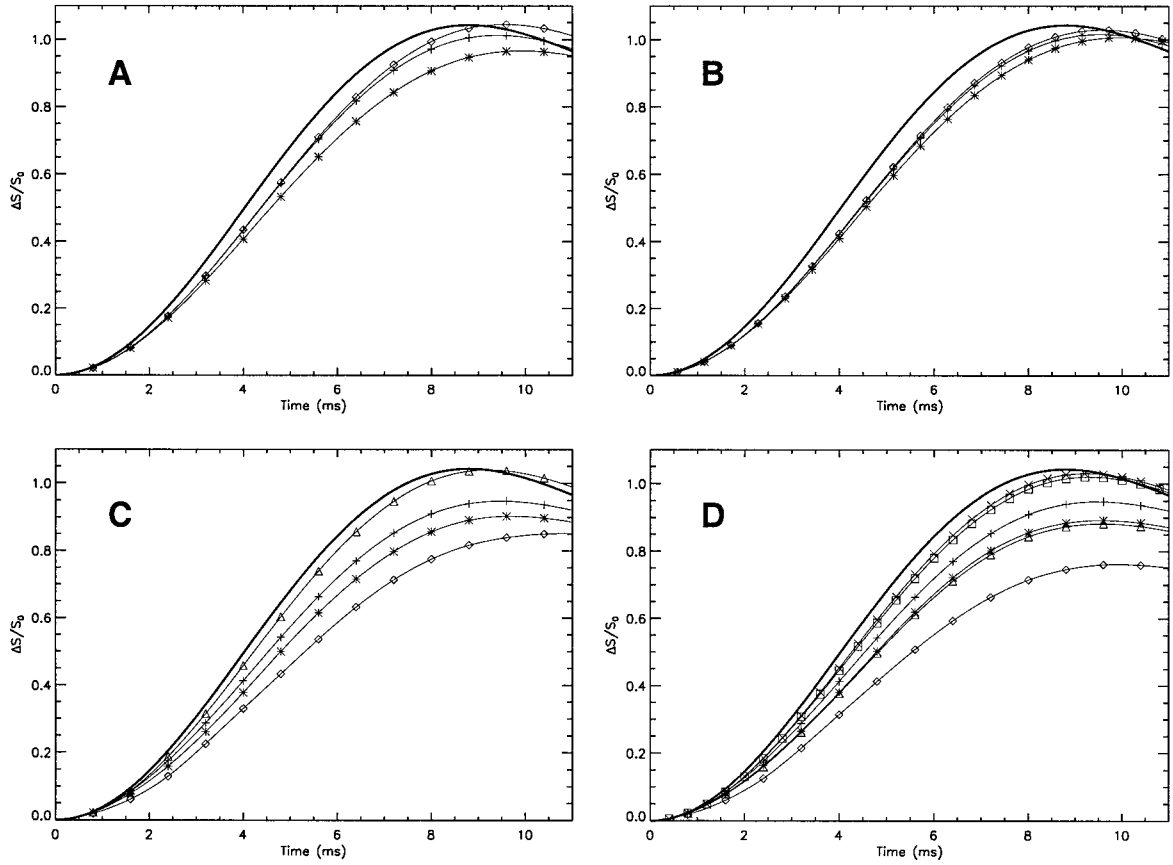

Figure 4. Simulated ^{15}N-^{13}C REDOR ($\Delta S/S_0$) plots employing the dipolar coupling value observed in glycine, $d_{NC} = 190$ Hz. Simulated data obtained for ideal δ pulses are given by the curves with the thicker linewidth. ^{13}C CSA parameters employed were $(\sigma_{11}, \sigma_{22}, \sigma_{33}) = (-73.1, 2.5, 70.5)$ ppm, ^{15}N was assumed to have no CSA as it is negligible in glycine. For simulation purposes, to obtain the ^{13}C resonance offsets for different crystallite orientations, we have assumed that the principal axes systems of the ^{15}N and ^{13}C chemical shift tensors coincide. As the integrated intensity of the REDOR signal is orientation independent, the orientation of the ^{15}N-^{13}C dipolar vector was assumed to be parallel to the main axis of the ^{15}N chemical shift tensor. Solid lines are splines fitted through the individual theoretically obtained data points. (A) and (B) Show the effect of different phasing schemes on the observed REDOR dephasing curves. (A) REDOR plots obtained at a spinning speed of 5000 Hz with 80 μs cagauss pulses at a power level of 50 kHz employing xx (+), $x\bar{x}$ (◊) and xy (*) phasing schemes. (B) REDOR plots obtained at a spinning speed of 7000 Hz with 40 μs tanh/tan pulses at a power level of 44 kHz employing xx (+), $x\bar{x}$ (◊) and xy (*) phasing schemes. (C) REDOR plots obtained with rectangular 180° pulses ($\chi = 0.1$), at a spinning speed of 5000 Hz and with RF field strengths of 50 (+), 48 (*) and 45 kHz (◊). The REDOR dephasing curve corresponding to a 40 μs tanh/tan adiabatic pulse with an RF field strength of 44 kHz and above is also given (Δ). (D) REDOR plots obtained with rectangular 180° pulses ($\chi = 0.1$), at a spinning speed of 5000 Hz and with 50 kHz RF field strength (+), 47.5 kHz RF field strength and 2 kHz resonance offset (*), 45 kHz RF field strength and 2 kHz offset (◊) and 47.5 kHz RF field strength and 4 kHz offset (Δ). The REDOR dephasing curves corresponding to a 40 μs tanh/tan adiabatic pulse, 44 kHz RF field strength with 10 kHz resonance offset (□) and 48 kHz RF field strength with 4 kHz offset (×) are also given.

in-house written programs. Initial simulations were performed with conventional powder averaging over ∼33 000 crystallite orientations as in our earlier studies (Leppert et al., 2000a, b, 2001; Heise, 2001; Leppert, 2001; Heise et al., 2001). The current version of our programs employs the efficient powder averaging scheme 'REPULSION' of Bak et al. (1997) requiring only ∼8000 crystallite orientations. All calculated FIDs contained negligible imaginary contributions and hence only the initial amplitude of the real part of the signal is considered in the simulations. To assess the relative performance of the adiabatic and rectangular inversion pulses, we have also calculated the REDOR response with rectangular inversion pulses employing the xy-4 phasing scheme. The rectangular pulses are divided into a finite number of time slices of 0.5 μs duration and the REDOR response is calculated as for the shaped pulses. For inversion pulses applied at the middle and end of a rotor cycle, the propagators (for

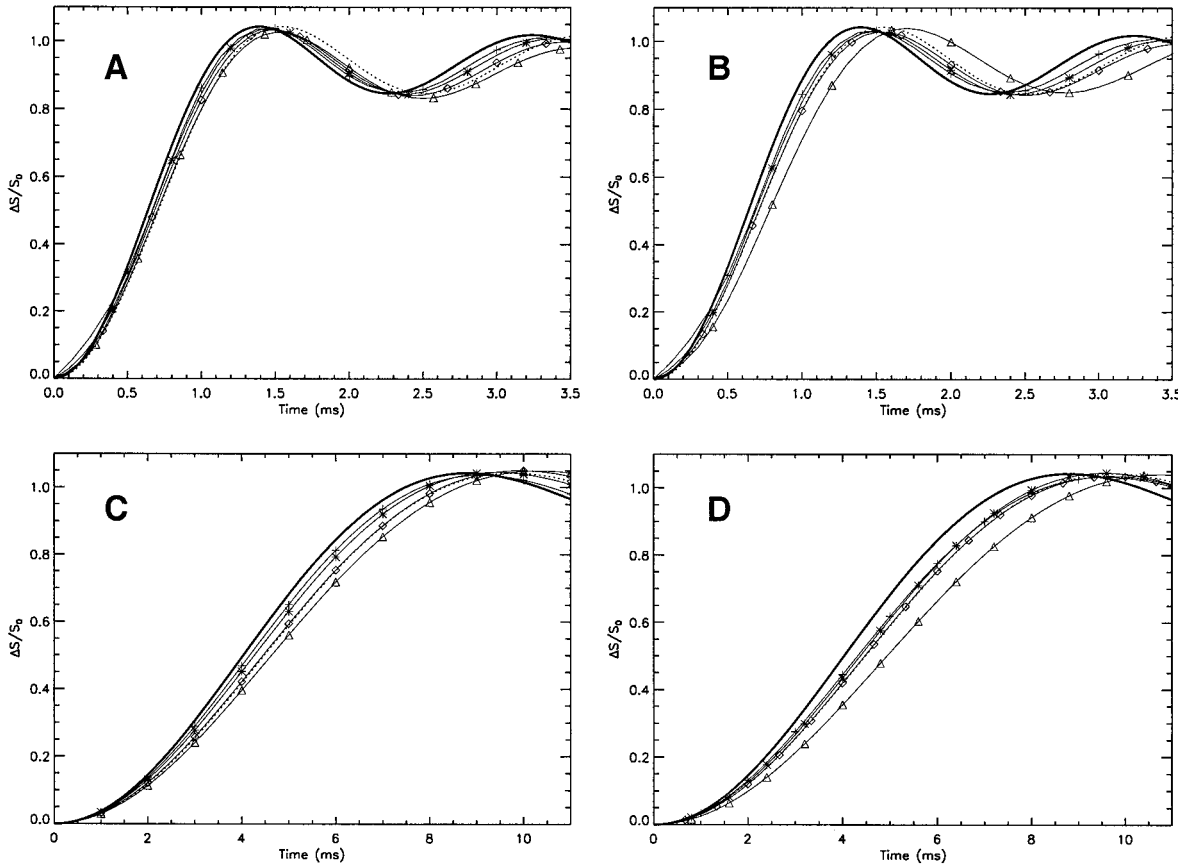

Figure 5. Simulated ^{15}N-^{13}C REDOR ($\Delta S/S_0$) plots employing dipolar coupling values observed in AibAib, d_{NC} = 1200 Hz (A, B) and glycine, d_{NC} = 190 Hz (C, D) with different adiabatic pulse shapes. Simulated data obtained for ideal δ pulses and with correct dipolar coupling value are given by the curves with the thicker linewidth. Ideal curves with 10% less dipolar coupling strength than the correct value are shown by dotted lines (- - -). (A) 40 μs tanh/tan pulses at a power level of 44 kHz and at spinning speeds of 4000 (+), 5000 (*), 6000 (◊) and 7000 Hz (Δ). corresponding to χ values of 0.32, 0.4, 0.48 and 0.56, respectively. (B) 80 μs cagauss pulses at a power level of 50 kHz and at spinning speeds of 4000 (+), 5000 (*) and 6000 Hz (◊) corresponding to χ values of 0.64, 0.8 and 0.96, respectively, and 70 μs tanh/tan pulses at a power level of 35 kHz at a spinning speed of 5000 Hz (Δ, χ = 0.7). (C) Plots at a spinning speed of 4000 Hz employing tanh/tan pulses of (+) 40 μs, χ = 0.32 and 44 kHz RF power, (∗) 50 μs, χ = 0.4 and 39.3 kHz RF power, (◊) 60 μs, χ = 0.48 and 39.3 kHz RF power and (Δ) 70 μs duration, χ = 0.56 and 35 kHz RF power. (D) 80 μs cagauss and 70 μs tanh/tan pulses, with parameters as in (B). Solid lines are splines fitted through the individual theoretically obtained data points. ^{15}N and ^{13}C CSA parameters of $(\sigma_{11}, \sigma_{22}, \sigma_{33}) = (-69.3, -30.6, 99.9)$ ppm and (92.1, 191.4, 239.1) ppm, respectively, were employed to generate the plots given in A and B. ^{13}C parameters employed in C and D were $(\sigma_{11}, \sigma_{22}, \sigma_{33}) = (-73.1, 2.5, 70.5)$ ppm, ^{15}N was assumed to have no CSA as it is negligible in glycine. For simulation purposes, to obtain the ^{13}C resonance offsets for different crystallite orientations, we have assumed that the principal axes systems of the ^{15}N and ^{13}C chemical shift tensors coincide. As the integrated intensity of the REDOR signal is orientation independent, the orientation of the ^{15}N-^{13}C dipolar vector was assumed to be parallel to the main axis of the ^{15}N chemical shift tensor.

all required RF pulse phases) are calculated separately and are reused in the REDOR calculation.

Experimental

All experiments were performed at room temperature on a 500 MHz wide bore Varian $^{\text{UNITY}}$*INOVA* solid state NMR spectrometer equipped with a 5 mm DOTY supersonic triple resonance probe and a waveform generator for pulse shaping. Cross-polarization under Hartmann–Hahn matching conditions was employed and the spectra were collected under high power ^{1}H TPPM decoupling of ∼89 kHz (Bennett et al., 1995). Typical ^{1}H, ^{13}C and ^{15}N 90° pulse widths were 2.8, 4.5 and 7.6 μs, respectively. ^{15}N-^{13}C REDOR (Figure 1) measurements were carried out employing samples of the dipeptide (^{13}C′,^{15}N)Aib-(^{15}N)Aib-NH$_2$ (Aib = α-aminoisobutyric acid) and of (1-^{13}C,^{15}N) glycine. In a fully labelled sample weak intermolec-

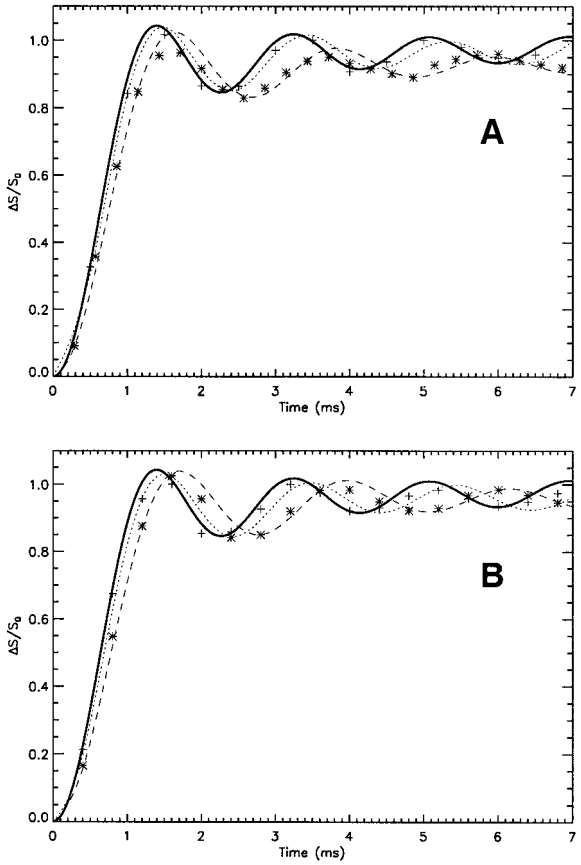

Figure 6. Experimental ^{15}N-^{13}C REDOR ($\Delta S/S_0$) data points obtained for the AibAib sample and *theoretical* REDOR dephasing curves (obtained from spline fitting of *theoretical* data points) for the corresponding pulse parameters. (A) 50 μs tanh/tan pulses at a RF power level of 39.3 kHz and at spinning speeds of 4000 (+, dotted lines, $\chi = 0.4$) and 7000 Hz (*, dashed lines, $\chi = 0.7$). (B) Plots at a spinning speed of 5000 Hz employing 80 μs cagauss pulses at a power level of 50 kHz (+, dotted lines, $\chi = 0.8$) and 70 μs tanh/tan pulses at a RF power level of 35 kHz (*, dashed lines, $\chi = 0.7$). Simulated data for ideal δ pulses is given by the curve with the thicker linewidth.

ular ^{13}C···^{15}N dipolar couplings can contribute to the observed REDOR dephasing when the dipolar recoupling period is large. To minimise such contributions, labelled samples are generally diluted with unlabelled molecules. (1-^{13}C, ^{15}N) glycine displays a two-bond ^{13}C-^{15}N dipolar coupling of ∼190 Hz and hence, this sample has been diluted with unlabelled glycine in the ratio of 1:10, as has been done in the earlier study of Jaroniec et al. (2000). Sample dilution would, in principle, also improve the accuracy of the measured REDOR distances even when one is dealing with significantly large dipolar couplings, as in the case of the dipeptide sample studied here ($d_{NC} \sim 1200$ Hz). For

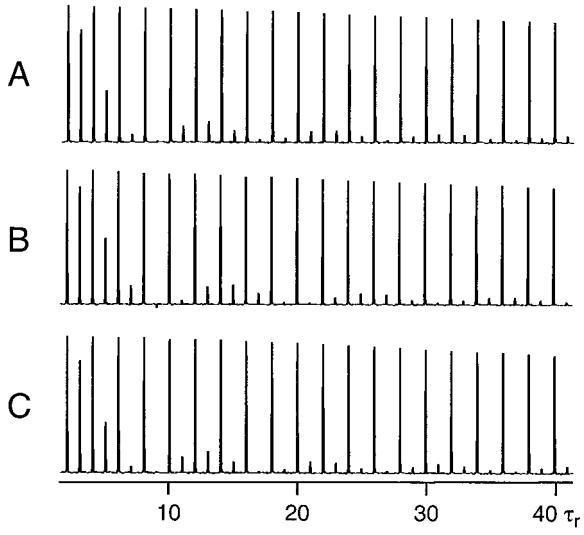

Figure 7. ^{15}N-^{13}C REDOR spectra of AibAib (centre band, 5000 Hz spinning speed) as a function of the dipolar dephasing time in steps of two rotor periods, without and with the application of the dephasing pulses. (A) 40 μs tanh/tan pulses, (B) 70 μs tanh/tan pulses, (C) 80 μs cagauss pulses.

shorter dephasing times, which are only typically required for the measurement of large dipolar couplings, the influence from intermolecular dipolar couplings is expected to be minimal. Hence, we have performed our REDOR studies on the dipeptide only with undiluted sample. The samples, approx. 35 mg each, were packed into small cylindrical inserts so as to fill ∼50% of the central rotor volume.

Results and discussion

To assess the effect of different pulse phasing schemes in REDOR experiments carried out with adiabatic inversion pulses, we have carried out numerical simulations (Figures 4A and 4B) of ^{15}N-^{13}C REDOR dephasing curves at spinning speeds in the range of 4000–7000 Hz using a typical two-bond ^{15}N-^{13}C dipolar coupling of 190 Hz. Signal intensities without (S_0) and with the application of the dephasing pulses (S) were calculated using the parameters given in the figure caption of Figure 4 which shows a few representative plots of $(S_0 - S)/S_0 = \Delta S/S_0$. Data corresponding to the ideal situation (δ 180° pulses) are also presented. In view of the excellent inversion profile of the adiabatic pulses, (Figures 2 and 3), we have not assessed exhaustively the efficacy of REDOR with different inversion pulse phasing schemes. Only

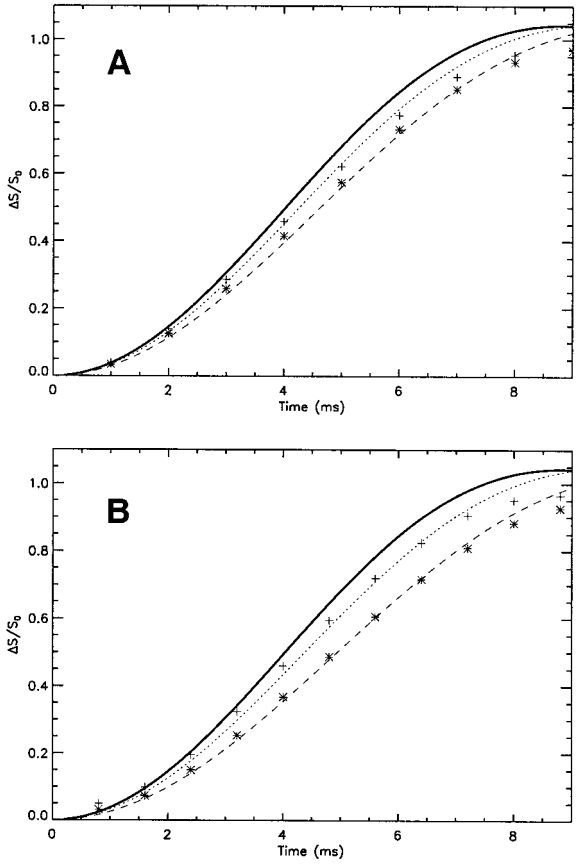

Figure 8. Experimental ^{15}N-^{13}C REDOR ($\Delta S/S_0$) data points obtained for the glycine sample and *theoretical* REDOR dephasing curves (obtained from spline fitting of *theoretical* data points) for the corresponding pulse parameters. (A) Plots at a spinning speed of 4000 Hz employing tanh/tan pulses of 50 μs (+, dotted lines, $\chi = 0.4$) and 70 μs duration (*, dashed lines, $\chi = 0.56$). (B) Plots at a spinning speed of 5000 Hz employing 80 μs cagauss pulses (+, dotted lines, $\chi = 0.8$) and 70 μs tanh/tan pulses (*, dashed lines, $\chi = 0.7$). Simulated data for ideal δ pulses is given by the curve with the thicker linewidth.

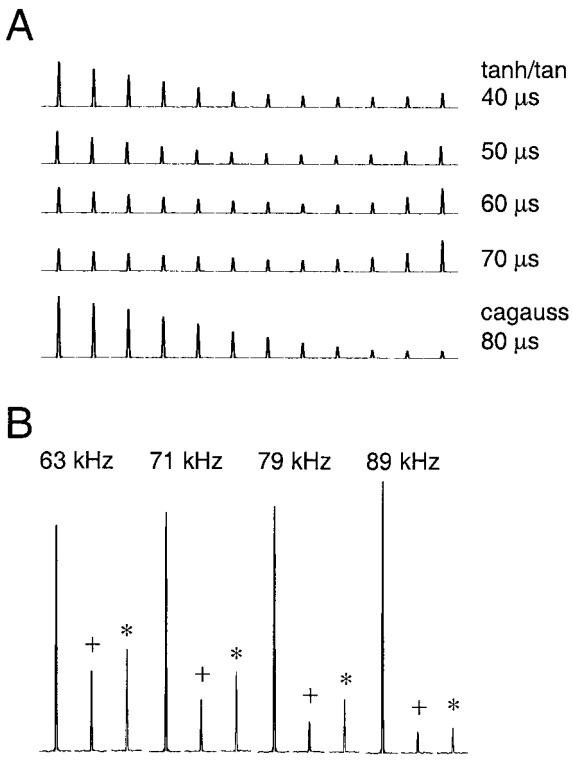

Figure 9. (A) Effect of adiabatic pulse power level on the dephased ^{15}N-^{13}C REDOR signal intensity of the glycine sample. The adiabatic pulse power level were varied from 40 to 51 dB, in steps of 1 dB (51 dB corresponds to an RF field strength of ~55.5 kHz). Spectra (without ^{15}N background subtraction) were collected at a spinning speed of 5000 Hz after 44 rotor periods with ^{1}H decoupling power of ~89 kHz. (B) Effect of ^{1}H decoupling power on the ^{15}N-^{13}C REDOR signal intensity of the glycine sample. Spectra (without ^{15}N background subtraction) were collected at a spinning speed of 5000 Hz, after 44 rotor periods, without and with the application of 40 μs tanh/tan adiabatic dephasing pulses. ^{1}H decoupling power levels are indicated on top of the spectra and ^{13}C power levels were ~49.5 kHz (+) and ~55.5 kHz (*).

the RF pulse phasing schemes such as xx, $x\bar{x}$ and xy that are typically employed with rectangular inversion pulses were analysed in the current investigation. The plots given in Figures 4A and 4B show the initial build-up region of the dephasing curves obtained with the different phasing schemes. From these plots it is seen that the deviation from the ideal curve is slightly larger with the xy phasing scheme and the $x\bar{x}$ phasing scheme has been uniformly employed in all simulations and experimental data given hereafter. In Figures 4C and 4D we have compared the relative REDOR performance seen with rectangular and adiabatic inversion pulses. A spinning speed of 5000 Hz and a dipolar coupling strength of 190 Hz were employed in generating these plots. The ^{13}C and ^{15}N CSA parameters employed in Figures 4A and 4B were also used for generating the plots. The dephasing curves for the rectangular 180° pulses were obtained employing xy-4 phasing schemes. It is seen from the simulations given here that when the CSA of the dephased spins is large, even for $\chi = 0.1$ the REDOR dephasing curve obtained for the rectangular 180° pulses deviates substantially from the ideal curve (Figures 4C and 4D). In the presence of H_1 inhomogeneity and resonance offset, albeit the xy-4 phasing scheme employed, this deviation gets worsened further. These plots suggest that reliable estimation of distances with conventional rectangular pulses would require a knowledge of the H_1 inhomogeneity distribution and its incorporation

into the REDOR calculation. Figures 4C and 4D also show a few typical REDOR dephasing curves obtained with a 40 μs tanh/tan pulse. The superior performance of the adiabatic inversion pulses can be clearly seen from our simulations.

To assess the dependence of the observed REDOR dephasing curves on χ, ^{15}N-^{13}C REDOR numerical simulations (Figure 5) were carried out at spinning speeds in the range of 4000–7000 Hz using typical one- and two-bond ^{15}N-^{13}C dipolar couplings of 1200 (A, B) and 190 Hz (C, D). Signal intensities without (S_0) and with the application of the dephasing pulses (S) were calculated using the parameters given in the figure caption of Figure 5 which shows a few representative plots of $(S_0 - S)/S_0 = \Delta S/S_0$. Data corresponding to the ideal situation (δ 180° pulses) are also presented. These plots reveal the dependence of the observed REDOR dephasing curves on χ and on the nature of the adiabatic pulse profile. χ variations were achieved either by changing the spinning speed at a given pulse width or by changing the pulse width at a given spinning speed. The dipolar oscillation frequency and the amplitude are seen to change with χ. For a given pulse shape, the deviation of the adiabatic pulse REDOR dephasing curve from the ideal curve increases with larger values of χ. For large values of χ, data analysis under a delta pulse approximation would result in dipolar coupling estimates which are smaller than the real value. For tanh/tan adiabatic pulses, it is seen that for $\chi < 0.5$ this apparent dipolar coupling strength lies approximately within 10% of the actual value. The extent of deviation of the adiabatic pulse REDOR dephasing curve from the ideal curve depends not only on χ but also on the adiabatic pulse shape employed. For example, at 5000 Hz the REDOR dephasing curve generated for a 80 μs cagauss pulse ($\chi = 0.8$) is much closer to the ideal curve than the curve generated for a 70 μs tanh/tan ($\chi = 0.7$) pulse (Figures 5B and 5D).

The efficacy of REDOR with adiabatic inversion pulses and the effects of the adiabatic pulse shape and duration on the REDOR dephasing curves have also been confirmed experimentally by ^{15}N-^{13}C REDOR measurements. These were carried out on samples of the dipeptide (^{13}C′,^{15}N) Aib-(^{15}N) Aib-NH_2 and of (1-^{13}C,^{15}N) glycine with dipolar couplings d_{NC} of ∼1200 Hz (Heise, 2001) and ∼190 Hz (Jaroniec et al., 2000), respectively. In Figure 6, we show representative experimental $\Delta S/S_0$ data obtained with the dipeptide sample employing tanh/tan and cagauss adiabatic pulse profiles. Figure 6 also shows the corresponding theoretical REDOR dephasing curves obtained employing a dipolar coupling strength of 1200 Hz and the adiabatic pulse parameters used in the experiment. Figure 7 shows a few spectra obtained employing different adiabatic inversion pulses. These experiments were performed with $x\bar{x}$ phase cycling of the adiabatic pulses. As seen in Figure 6, the experimentally measured $\Delta S/S_0$ ratios are in good agreement with those expected from numerical simulations. Figure 8 shows a few representative experimental $\Delta S/S_0$ data obtained with the glycine sample employing adiabatic pulses. The contribution to the experimental ^{15}N signal intensity arising from the ^{15}N background of the unlabelled sample has been subtracted in these plots. The theoretical REDOR dephasing curves generated employing a dipolar coupling strength of 190 Hz and the corresponding adiabatic pulse parameters used in the experiment are also given in Figure 8. At short dephasing times, as with the dipeptide sample, one sees a satisfactory fit between the experimental data and the simulated curves. At longer dephasing times the fit appears not to be very satisfactory although all experiments with adiabatic pulses have been carried out employing RF power levels satisfying the adiabatic threshold requirements. For example, for the 40 μs tanh/tan pulse we have employed an RF power level of ∼44 kHz, the minimum required to achieve good spin inversion (Figure 2). The optimal RF power needed for the adiabatic pulses was also determined experimentally by monitoring the REDOR dephasing as a function of the adiabatic pulse power level. Although the usage of higher RF power levels would still result in good spin inversion and would also ensure that the RF field strength throughout the whole sample volume is above the minimum threshold required, we have essentially employed the minimum required RF power levels for the adiabatic pulses. Application of the adiabatic pulses at high RF power levels lead to degradation in the dipolar recoupling efficiency due to the cross talk between the ^{1}H decoupling and ^{13}C irradiation (Ishii et al., 1995; Nishimura et al., 2001; Jaroniec et al., 2001). This degradation becomes severe for pulses with a high duty factor. This is shown in Figure 9. Figure 9A shows the observed REDOR dephased signal intensity with different adiabatic pulses as a function of the adiabatic pulse power employed. Figure 9B shows the effect of the decoupler power level on the intensity of the observed REDOR signal obtained with 40 μs tanh/tan pulses. As has been noted in the literature and as seen from Figure 9, insufficient proton decoupling power, in relation to the RF power

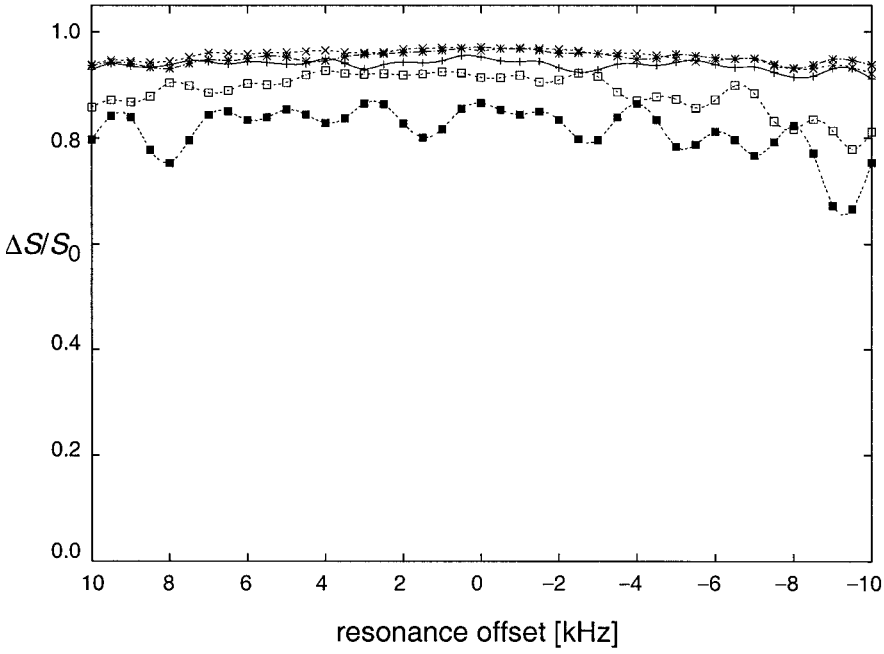

Figure 10. Dependence of $\Delta S/S_0$ on the ^{13}C carrier offset in the ^{15}N-^{13}C REDOR experiment on glycine with different inversion pulses (36 rotor periods of dipolar recoupling at 4000 Hz spinning speed, the ^{15}N background signal has been subtracted). The carrier offset is referenced to the ^{13}C isotropic frequency and is varied in steps of 0.5 kHz over a range of ±10 kHz from the isotropic position. The inversion pulses employed were 40 μs tanh/tan pulses with ∼44 kHz RF power (+), 70 μs tanh/tan pulses with ∼35 kHz RF power (×), 80 μs cagauss pulses with ∼50 kHz RF power (*), 9 μs rectangular 180° pulses with 55.5 kHz RF power and xy-4 phasing (□) and 9.9 μs rectangular 180° pulses with 55.5 kHz RF power and xy-4 phasing (■).

employed in the ^{13}C channel, can significantly affect REDOR recoupling. The maximum decoupling power level employed here was ∼89 kHz. With the availability of higher ^{1}H decoupling field strengths in the current generation of MAS probes, however, it should be feasible to execute REDOR experiments with sufficient ^{1}H/^{13}C RF power mismatch and obtain accurate distance estimates. The effect of insufficient RF power mismatch becomes critical at longer mixing times and insufficient RF mismatch in our experiments is probably the main reason for the unsatisfactory fit seen between the experimental and simulated data at longer mixing times (Figure 8).

For making resonance assignments in uniformly labelled systems, 2D chemical shift correlation techniques are found to be useful. As mentioned earlier, dipolar recoupling experiments such as TEDOR and RFDR can be conveniently employed for this purpose. An effective implementation of these experiments requires a good, offset independent dipolar recoupling performance. In Figure 10 we show for the glycine sample the effect of ^{13}C carrier offset on the observed ($\Delta S/S_0$) ratio. For comparison, corresponding data obtained employing rectangular 180° pulses (with xy-4 phasing scheme) are also given. As expected (Figure 4), the performance of the rectangular pulses, in spite of their much shorter duration, is seen to be inferior to the performance of the adiabatic pulses, both on- and off-resonance. It is also seen that errors in the 180° pulse width calibration (or the presence of H_1 inhomogeneity) can affect significantly the observed dipolar recoupling characteristics with rectangular 180° pulses. The effects of large CSAs are not eliminated at a spinning speed of 4 kHz and rectangular 180° pulses with durations typically employed in REDOR studies do not have sufficient inversion bandwidth. Under these circumstances, in agreement with earlier studies (Jaroniec et al., 2001), the present investigations also reveal that the xy-4 phasing scheme does not compensate for variations in the resonance offset arising from large CSAs. In principle, one can avoid the effect of CSA on the REDOR dephasing by using the spin with the large CSA as the observed spin. However, this may not always be advantageous; for example, when the spin with the large CSA, say ^{13}C′, is dipolar coupled with several ^{15}N spins with well resolved isotropic chemical shifts (Leppert et al., 2000a). In this situation, it is easier to extract ^{13}C-^{15}N

distances by doing a ^{15}N-^{13}C REDOR. In a ^{13}C-^{15}N REDOR experiment with ^{13}C as the observed spin, all ^{15}N spins contribute to the observed REDOR dephasing which would make data analysis difficult. On the other hand, the ^{15}N-^{13}C REDOR data can be analysed with a two spin approximation. The effects of large CSA can also be eliminated by high speed spinning. However, especially at high H_0 fields, this may become difficult in the study of some biological systems, e.g., membrane bound peptides or proteins. At moderate spinning speeds and when the dephased spins have large CSA, it is necessary to have 180° pulses with large inversion bandwidth. Our studies show that adiabatic pulses can be employed to meet this requirement. Additionally, in biological systems, it may not be desirable to restrict the sample volume in order to improve H_1 inhomogeneity. As much of the rotor volume may be occupied, e.g., by lipids and water, restricting the sample volume would lead to considerable loss in the signal to noise ratio. In situations where a good tolerance to H_1 inhomogeneity is required, adiabatic pulses offer an attractive means to reduce H_1 inhomogeneity effects in REDOR experiments.

In conclusion, from our studies at moderate spinning speeds, it is seen that even when the adiabatic pulses occupy a significant fraction of the rotor period, it is feasible to achieve efficient REDOR recoupling of dipolar interactions. Although a few REDOR studies have been reported in the literature at high spinning speeds (Jaroniec et al., 2000; Chan et al., 2000), moderate spinning speeds in the range of 3–6 kHz may suffice in situations where the observed spins do not have much CSA. Moderate spinning speeds may also be required to reduce average power dissipation in the probe at large dephasing times. At moderate spinning speeds, when the dephased spins have a large CSAs, our studies clearly show that one can obtain superior dipolar recoupling performance by taking recourse to adiabatic inversion pulses instead of conventional rectangular 180° pulses. The satisfactory agreement between numerical simulations and experimental results reported here suggests that by taking into account explicitly the χ dependence in the data analysis one can obtain accurate distance estimates from REDOR data generated with adiabatic inversion pulses. The extraction of structural data from experimental adiabatic pulse REDOR dephasing curves would involve the following steps: (1) Obtaining an initial estimate of the apparent dipolar coupling strength assuming δ 180° pulses, (2) generation of a series of simulated REDOR dephasing curves for different dipolar coupling values (around the estimated apparent dipolar coupling strength) using the adiabatic inversion pulse parameters employed in the experiment and (3) comparison of the experimental and simulated curves to obtain the best fitting dipolar coupling strength. Although the extraction of exact distance information from REDOR data collected with adiabatic inversion pulses may become time consuming, it is a price that is worth paying for eliminating resonance offset and H_1 inhomogeneity effects and hence for obtaining reliable distance estimates. However, it is possible to avoid such a detailed procedure and still obtain estimates of dipolar coupling strengths within an error of less than 10% with adiabatic pulses. This can be achieved, for example, in the case of tanh/tan pulses with $\chi < 0.5$. Similar to the usage of adiabatic inversion pulses in heteronuclear dipolar recoupling experiments reported here, we are currently assessing the performance of the RFDR pulse scheme with adiabatic inversion pulses. The results of these investigations will be reported elsewhere.

References

Bak, M. and Nielsen, N.C. (1997) *J. Magn. Reson.*, **125**, 132–139.

Baum, J., Tycko, R. and Pines, A. (1985) *Phys. Rev.*, **A32**, 3435–3447.

Bennett, A.E., Griffin, R.G. and Vega, S. (1994) *NMR Basic Principles and Progress*, Springer Verlag, Berlin, **33**, 1–77.

Bennett, A.E., Ok, J.H., Griffin, R.G. and Vega, S. (1992) *J. Chem. Phys.*, **96**, 8624–8627.

Bennett, A.E., Rienstra, C.M., Auger, M., Lakshmi, K. V. and Griffin, R.G. (1995) *J. Chem. Phys.*, **103**, 6951–6958.

Bennett, A.E., Rienstra, C.M., Griffiths, J .M., Zhen, W., Lansbury, P.T. and Griffin, R.G. (1998) *J. Chem. Phys.*, **108**, 9463–9479.

Chan, J.C.C. and Eckert, H. (2000) *J. Magn. Reson.*, **147**, 170–178.

Dusold, S. and Sebald, A. (2000) *Annu. Rep. NMR Spectrosc.*, **41**, 185–264.

Fujiwara, T., Sugase, K., Kainosho, M., Ono, A., Ono, A.M. and Akutsu, H. (1995) *J. Am. Chem. Soc.*, **117**, 11351–11352.

Goetz, J.M. and Schaefer, J. (1997) *J. Magn. Reson.*, **127**, 147–154.

Griffin, R.G. (1998) *Nat. Struct. Biol.*, **5**, 508–512.

Gullion, T. and Schaefer, J. (1989b) *Adv. Magn. Reson.*, **13**, 57–83.

Gullion, T. and Schaefer, J. (1989a) *J. Magn. Reson.*, **81**, 196–200.

Gullion, T. and Schaefer, J. (1991) *J. Magn. Reson.*, **92**, 439–442.

Gullion, T., Baker, D.B. and Schaefer, J. (1990) *J. Magn. Reson.*, **89**, 479–484.

Heise, B. (2001) Ph.D. thesis, Friedrich-Schiller-Universität, Jena.

Heise, B., Leppert, J. and Ramachandran, R. (2000) *J. Magn. Reson.*, **146**, 181–187.

Heise, B., Leppert, J., Wenschuh, H., Ohlenschläger, O., Görlach, M. and Ramachandran, R. (2001) *J. Biomol. NMR*, **19**, 167–179.

Hing, A.W., Vega, S. and Schaefer, J. (1992) *J. Magn. Reson.*, **96**, 205–209.

Hing, A.W., Vega, S. and Schaefer, J. (1993) *J. Magn. Reson.*, **103**, 151–162.

Hwang, T., van Zijl, P.C.M. and Garwood, M. (1998) *J. Magn. Reson.*, **133**, 200–203.
Ishii, Y., Ashida, J. and Terao, T. (1995) *Chem. Phys. Lett.*, **246**, 439–445.
Jaroniec, C.P., Tounge, B.A., Herzfeld, J. and Griffin, R.G. (2001) *J. Am. Chem. Soc.*, **123**, 3507–3519.
Jaroniec, C.P., Tounge, B.A., Rienstra, C.M., Herzfeld, J. and Griffin, R.G. (2000) *J. Magn. Reson.*, **146**, 132–139.
Kupce, J. and Freeman, R. (1995) *J. Magn. Reson.*, **A117**, 246–256.
Kupce, J. and Freeman, R. (1996) *J. Magn. Reson.*, **A118**, 299–303.
Leppert, J. (2001) Ph.D. thesis, Friedrich-Schiller-Universität, Jena.
Leppert, J., Heise, B. and Ramachandran, R. (2000a) *J. Magn. Reson.*, **145**, 307–314.
Leppert, J., Heise, B. and Ramachandran, R. (2000b) *J. Biomol. NMR*, **18**, 153–164.
Leppert, J., Heise, B. and Ramachandran, R. (2001) *Solid State NMR*, **19**, 1–18.
McDermott, A., Polenova, T., Bockmann, A., Zilm, K. W., Paulsen, E.K., Martin, R.W. and Montelione, G.T. (2000) *J. Biomol. NMR*, **16**, 209–219.
Naito, A., Nishimura, K., Kimura, S., Tuzi, S., Aida, M., Yasuoka, N. and Saito, H. (1996) *J. Phys. Chem.*, **100**, 14995–15004.
Nishimura, K., Fu, R. and Cross, T.A. (2001) *J. Magn. Reson.*, **152**, 227–233.
O'Connor, R.D. and Schaefer, J. (2002) *J. Magn. Reson.*, **154**, 46–52.
Pauli, J., von Rossum, B., Förster, H., de Groot, H.J.M and Oschkinat, H. (2000) *J. Magn. Reson.*, **143**, 411–416.
Tannus, A. and Garwood, M. (1996) *J. Magn. Reson.*, **A120**, 133–137.